

# Vibrational States of the Hydrogen Isotopes on Pd(111)

Steven W. Rick\*<sup>†</sup> and J.D. Doll

*Department of Chemistry*

*Brown University*

*Providence, RI 02912*

The ground and excited vibrational states for the three hydrogen isotopes on the Pd(111) surface have been calculated. Notable features of these states are the high degree of anharmonicity, which is most prominently seen in the weak isotopic dependence of the parallel vibrational transition, and the narrow bandwidths of these states, which imply that atomic hydrogen is localized on a particular surface site on time scales of 100 picoseconds or more. Experiments to resolve ambiguities concerning the present system are suggested.

---

\* Present address: Department of Chemistry, Columbia University, New York, NY 10027

<sup>†</sup> contact author, telephone: (212) 854-5650, fax: (212) 932-1289

Hydrogen atoms chemisorbed on a metal surface[1] display a variety of phenomena, ranging from localization on a particular binding site with thermally activated hopping or incoherent tunneling between the sites to extended band states, depending on the metal, the face, the temperature, and the coverage. A hydrogenic-band model in which the hydrogen wavefunction is delocalized parallel and localized perpendicular to the surface was first[2] proposed by Christmann, *et al.*, in 1979 for H on Ni(111)[3]. Puska and co-workers followed up on this suggestion by calculating the states for hydrogen on a rigid Ni surface[4]. They find narrow width ground states and excited states with appreciable width ( $\sim 50$  meV), particularly for the (110) and (111) face. Since then there has been a number of experiments which reported evidence of band-like states, mainly along the "troughs" of surfaces such as the (211) face of body-centered cubic (bcc) metals[5] and the (110) face of face-centered cubic (fcc) metals[6] or for the smoothly corrugated (111) face of fcc metals[7,8]. The helium scattering experiments of Hsu, *et al.* find a hydrogen phase with 6-fold symmetry[8]. The authors explain this phase in terms of hydrogen being quantum mechanically delocalized over two adjacent 3-fold sites on the sub-picosecond time scale of the helium scattering event. These results are for a hydrogen coverage of half saturation and a temperature range of 140 to 300 K and the same results are seen for D as for H [9]. The time scales for hydrogen diffusion have been measured for several metal surfaces (Ni(100)[10], W(110)[11], Rh(111)[12], and Pt(111)[13]). At high temperatures, diffusion shows an Arrhenius dependence indicative of thermally activated hopping between localized sites, with activation energies ranging from 0.15 to 0.52 eV. At temperatures below 100 K, Gomer and coworkers[11] for H/W(110) and Zhu, *et al.*[14], for H/Ni(100) find a diffusion rate due to tunneling which is independent of temperature. The diffusion rates at the low temperatures are very small ( $10^{-11}$  to  $10^{-13}$  cm<sup>2</sup>/sec), indicating very little wavefunction overlap between adjacent sites and bandwidths of  $10^{-2}$  to  $10^{-11}$  meV [15].

The small bandwidth for H on Ni(100) is consistent with the band calculations of Puska and co-workers[4] and high resolution electron-energy loss spectroscopy (HREELS) experiments[16].

Vibrational spectroscopy such as HREELS provides a direct experimental probe of the nature of the hydrogen states. HREELS gives direct evidence as to whether vibrational excitations correspond to small vibrations about an equilibrium position as is typically the case (e.g. H/Ni(100)) or correspond to transitions to broad bands (H/Cu(110)). An HREELS study of H/Pd(111) at high coverages (a hydrogen exposure of 2 Langmuirs) shows two narrow peaks: a parallel vibration at  $774\text{ cm}^{-1}$  and a perpendicular vibration at  $998\text{ cm}^{-1}$ [17]. In this letter we report the vibrational states for the three isotopes of hydrogen on Pd(111) in the single adatom limit. The low coverage limit presents the best conditions for delocalized states, since the H-H interaction is expected to be purely repulsive. Increasing coverage should lead to a higher probability of localized states. This supposition is borne out by experiment, in which evidence of quantum delocalization disappears at high coverages [6,8]. Furthermore, although the widths of the excitations can vary with coverage, the position of the peak center does not have a strong coverage dependence.

In the present computations, the lattice is kept rigid in the minimum energy configuration of the surface in the absence of any adsorbates. The magnitude of adsorbate induced reconstructions is examed below. The clean surface does not reconstruct, the top surface only contracts by  $0.07\text{ \AA}$  relative to the bulk lattice spacing. The (111) surface is a hexagonal surface with 2 distinct sites: a tetrahedral site directly above a subsurface atom and an octahedral site, over a metal atom in the second subsurface layer. The two sites are treated as fully degenerate since the potential used predicts them to be energetically equivalent. The interaction potential is taken to be the Embedded Atom Method (EAM) potential of Daw and Baskes [18]. The EAM potential has a form borrowed from density functional theory and is determined by fitting to properties of the bulk system. Although this potential contains only bulk

data, it successfully reproduces the phase diagram for H/Pd(111)[19] and predicts the heat of absorption of hydrogen to be 2.85 eV, which is the experimental value[20]. This predicted value is the classical binding energy relative to an isolated atom and is for hydrogen absorbed on the rigid surface. Lattice relaxations lower the energy an additional 0.077 eV. The EAM barrier for surface diffusion is 175 meV. This barrier is not known experimentally but the barrier to bulk diffusion is 226 meV[21]. EAM predicts 152 meV for the bulk barrier, allowing for relaxation of the palladium atoms.

To find the vibrational states, we use the tight-binding approximation in which we calculate states localized on a particular binding site and take the appropriate linear combinations to construct states with the full 2-dimensional periodicity of the surface (see, e.g., Ref. [22]). The full periodic Hamiltonian of our system,  $\mathcal{H}$ , is written as a localized part,  $\mathcal{H}_0$ , plus the corrections,  $\Delta U$ . In the localized Hamiltonian, the hydrogen only interacts with the nearest three surface palladium atoms and the nearest three subsurface palladium atoms. These six interactions most nearly reproduce the full potential of the lattice in the region of the 3-fold site. Three eigenstates of  $\mathcal{H}_0$  are calculated: a ground state with  $A_1$  symmetry and excited states with  $A_1$  and E symmetries. The states are found by solving the Schrödinger equation on a 3-dimensional mesh of spacing 0.025 Å and—for the the excited states—simultaneously projecting out the lower energy states[23]. The accuracy of the ground and E states can be checked using the Diffusion Monte Carlo (DMC) method, which solves the Schrödinger equation exactly[24]. The E state can be calculated using the DMC method using the fixed-node approximation, since for the E-symmetry state the fixed node approximation is exact and the position of the nodal plane is easily deduced by symmetry. For the  $A_1$  state, the fixed-node approximation is not exact. The Bloch states,  $\Psi_{n,\mathbf{k}}$ , with  $\mathbf{k}$  the two-dimensional wavevector, are constructed by calculating the overlap between nearest neighbor surface sites only. The necessary overlap integrals can be easily done on the same mesh as is used to solve

for the localized states. The overlap integral between adjacent sites is less than 0.17, so the tight-binding approximation is reasonable.

The band centers and widths for the three lowest energy states are shown on Table I. The energies are all relative to the classical binding energy (-2.85 eV). The states for all three isotopes are very localized, the only states with a bandwidth larger than 1 meV are the H excited states. The width for each state narrows with increasing mass roughly as  $e^{-\sqrt{m}}$ [25].

In order to assist with spectroscopic assignments the  $\mathbf{k}=0$  H band-states are plotted along the three directions (Fig. 1). The left side of Fig. 1 shows the states' amplitude as a function of one surface coordinate, the  $[\bar{1}21]$  direction, and the  $[111]$  direction perpendicular to the surface, at a constant value for the other surface coordinate equal to the center of the unit cell. The right side shows the same wavefunctions as a function of the two surface coordinates at a constant height of 1 Å above the surface plane. The localized nature of the ground state is apparent. The excited state  $A_1^1$  is much broader and can be identified as predominantly a perpendicular vibrational excitation, since the nodal surface is nearly a plane parallel to the surface. The  $A_1^0$  to  $A_1^1$  transition will be dipole active in HREELS, the  $A_1^0$  to E transition can be seen only through impact scattering[26].

Table I also shows the energy differences between the ground and excited states for the parallel mode (the  $A_1^0$  to E transition) and the perpendicular mode ( $A_1^0$  to  $A_1^1$ ) for the three isotopes. Shown is the energy differences between the centers of the bands, although for the H isotope the excited states are broad enough that wide loss peaks might be detectable experimentally. The ordering of the vibrational peaks is the opposite of Conrad, *et al.*, who assign  $\omega_{\parallel}=774 \text{ cm}^{-1}$  and  $\omega_{\perp}=998 \text{ cm}^{-1}$  based on their HREELS experiments at high coverages [17]. The ordering of the parallel and perpendicular modes does vary for hydrogen on various metals and is a sensitive gauge of the metal-hydrogen interaction[1]. For examples with three-fold or quasi-three-fold coordination, H/Ru(0001) [27] and H/Ni(111) [28] have  $\omega_{\perp} > \omega_{\parallel}$  and H/Pt(111)[29]

and H/Rh(110)[30] have  $\omega_{\parallel} > \omega_{\perp}$ , although the H/Pt(111) assignment is challenged by Feibelman and Hamann [31]. If the experimental assignments for H/Pd(111) are correct, the EAM potential used here appears to misrepresent the relative stiffness of the two vibrations.

The isotope dependence of the computed frequencies is unusual and demonstrates the importance of anharmonic effects, particularly for the parallel frequency. The ratio of  $\omega_{\parallel}(\text{H})/\omega_{\parallel}(\text{D})$  is only 1.19, different from the  $\sqrt{2}$  dependence of harmonic vibrations. The ratio of  $\omega_{\perp}(\text{H})/\omega_{\perp}(\text{D})$  is 1.32, closer to  $\sqrt{2}$ . The anharmonic nature of the vibrational states can be seen by comparing the exact energies with harmonic estimates (Fig. 2). The band state energies (the longer horizontal line on the left) is shown connected (by the dotted line) to the harmonic estimate of the energy of that state (the smaller horizontal line on the right). The harmonic estimate is based on the curvature of the potential minimum of the absorbed state. Also visible in Fig. 2 are the bandwidths of the  $A_1^1$  and E states. All the states are lower in energy than the harmonic estimate. Most notable is the E state of H, which is lower by 90 meV or about 20%. That the vibrational frequencies are sensitive to features of the potential other than the curvature of the well bottom should be a warning to those who might attempt to construct potentials by fitting harmonic estimates to experimental values of the frequencies.

Most experimental spectra have a isotope dependence closer to  $\sqrt{2}$ , but the weak dependence of the parallel mode has precedence: HREELS experiments by Mate and Somorjai for H/Rh(111) find only a very small isotopic shift of about  $10 \text{ cm}^{-1}$  for a loss feature believed to be a transition to a delocalized band with E symmetry[7]. HREELS experiments for H and D on Ni(100)[32] and Rh(100)[33] have frequency ratios of the perpendicular mode close to  $\sqrt{2}$ , although overtones in the H/Rh(100) spectra show noticeable anharmonicities. For H and D on Pd(100) [34], the  $\omega_{\perp}$  ratio is about 1.3 and for the Ni(110) and Rh(110) surfaces the ratio are 1.25[35] and 1.35 [30], respectively. Calculations for H/Rh(0001) find isotope ratios for several states all in the range of 1.41 to 1.46 and

harmonic estimates differ from the anharmonic calculations by, at most, 8%[36].

The H/Pd(111) bandwidths are much narrower and the band gaps larger than those calculated for H/Ni(111)[4]. The ground state for that system has a width of 4 meV, the first excited state, which has E symmetry, has a width of 40 meV, and the next excited state, with A<sub>1</sub> symmetry, has a width of 74 meV. The larger widths of the Ni states is due to the lower diffusion barrier for H on Ni(111)[18] and the shorter lattice constant for Ni (3.52Å for Ni, 3.89 Å for Pd).

From the localized tight-binding states, estimates of both the magnitude of hydrogen induced reconstructions and time scales for hydrogen tunneling between adjacent surface sites can be made. As mentioned previously, lattice distortions lower the classical binding energy by 77 meV, as predicted by the EAM potential. This energy is a factor of ten larger than the largest bandwidth (Table I) and four orders of magnitude greater than the ground state width. Thus the small polaron condition is easily met: the energy gained from self-trapping the adsorbate by small lattice distortions is greater than the kinetic energy gained by forming extended bands[37]. Small polaron theory provides a convenient formalism for describing the tunneling process from site to site, including the influence of phonons. The small polaron Hamiltonian is found by expanding the potential around the rigid lattice potential,  $V^{rigid}(\mathbf{r})$ , to first order in the phonon coordinates,

$$V^{sp}(\mathbf{r}, \mathbf{Q}) = V^{rigid}(\mathbf{r}) + \sum_l V_l^a Q_l \quad (1)$$

where

$$V_l^a = \left. \frac{\partial V(\mathbf{r}, \mathbf{Q})}{\partial Q_l} \right|_{\mathbf{r}=\mathbf{r}^a},$$

$V(\mathbf{r}, \mathbf{Q})$  is the EAM potential energy,  $Q_l$  is the  $l^{th}$  perfect lattice (no adsorbate) phonon coordinate and  $\mathbf{r}^a$  is the hydrogen position of the minimum of  $V^{rigid}(\mathbf{r})$  at site "a". The small polaron Hamiltonian,  $\mathcal{H}_p$ , is

then the sum of the rigid lattice Hamiltonian,  $\mathcal{H}$ , a perfect lattice phonon part and the linear coupling between the two,

$$\mathcal{H}_p = \mathcal{H} + \sum_l \left( \frac{-\hbar^2}{2m_{Pd}} \nabla_l^2 + \frac{1}{2} m_{Pd} \omega_l^2 Q_l^2 \right) + \sum_l V_l^a Q_l \quad (2)$$

where  $m_{Pd}$  is the palladium mass and  $\omega_l$  the  $l^{th}$  phonon frequency. The H-phonon coupling will cause the phonon coordinates to be displaced by  $V_l^a/m_{Pd}\omega_l^2$ . The energy gained by the phonon displacements is  $E_{loc} = \sum (V_l^a)^2/2m_{Pd}\omega_l^2$ .

In the temperature regime where tunneling is the dominant mechanism for diffusion ( $T < 150-100$  K) only the ground state will be populated due to the large gap between the ground and excited states. The time scale,  $\tau_{ab}$ , for tunneling from the ground state of site "a" ( $\phi_a$ ) to any of the three nearest neighbor states "b" ( $\phi_b$ ) is given by

$$\tau_{ab}^{-1} = 3J_{ab}S_{ab}(T)/\hbar. \quad (3)$$

and is the product of the Hamiltonian matrix element between adjacent tight-binding states,  $J_{ab} = \langle \phi_a | \mathcal{H}_p | \phi_b \rangle$ , and a temperature dependent phonon overlap term,  $S_{ab}$ . The factor of three accounts for the number of nearest neighbor sites and the matrix element  $J_{ab}$  is equal to 1/6 the groundstate bandwidth [38]. Phonon coupling destroys some of the coherence of the bands, an effect which increases with temperature. At  $T=0$ ,

$$S_{ab}(T=0) = e^{-\sum_l \frac{1}{2} \left( \frac{m_{Pd}\omega_l}{2\hbar} \right) ((V_l^a - V_l^b)/m_{Pd}\omega_l)^2}.$$

Just considering the 24 phonon modes from the vibrations of the four atoms involved in the unit cell plus the four nearest neighbor surface atoms gives a  $E_{loc}$  of 46 meV. The localization energy is more than half the exact localization energy (77 meV) gained by relaxing the entire lattice, so the 24 phonon modes included here contain most of the important relaxation modes. The phonon displacements that give rise to this



localization are small. For the most strongly coupled mode (a symmetric stretch parallel to the surface of the three nearest Pd atoms), the phonon displacement,  $V_i^a/m_{Pd}\omega_i^2$ , is only 0.08 Å.

The time scale for tunneling from Equation (3) is  $2.6 \times 10^2$  ps for H,  $3.8 \times 10^4$  ps for D, and  $7.2 \times 10^5$  ps for T. The phonon overlap,  $S_{ab}(T=0)$ , is 0.46 and is only small modification on the tunneling matrix element. These time scales are all much longer than the sub-picosecond time scale needed to explain the Hsu, *et al.*, experiments within a quantum delocalization mechanism[8]. The calculated rates are the result of a model potential and are by no means exact, but there are a few reasons to believe that the tunneling time scales should be greater than 1 ps. Since both the diffusion barrier and the lattice constant for the Ni(111) surface are less than for Pd(111), the H/Pd(111) bands should be narrower than 4 meV, the calculated H/Ni(111) groundstate bandwidth [4]. This bandwidth, when inserted into Equation (3), gives a time scale of .3 ps (without phonon corrections); a narrower bandwidth would give localization on the helium scattering time scale. In addition, since the isotope dependence is so strong, the experimental results, if due to large bandwidths, should be different for H and D. The evidence for delocalization from the Hsu experiments is the symmetry change with decreasing coverage from 6-fold to 3-fold and the accompanying attenuation of the specular intensity. The delocalized states are deduced using a model for the helium scattering process in which the helium atoms scatter off a hydrogen density which in the plane of the surface is a constant value within an ellipsoid centered at the bridge site and a major semi-axis equal to 0.8Å and minor semi-axis equal to 0.5Å. Thus the hydrogen density has a constant value which spans both sides of the unit cell and the hydrogen is delocalized within the unit cell. This is a qualitatively different picture of the hydrogen wavefunction than the ground state shown in Fig. 1.

There are factors other than the accuracy of the EAM potential which are relevant in a comparison of the present calculations with the experiments of Hsu, *et al.* The experiments were done at a coverage of a half so hydrogen-hydrogen interactions might be an issue, although most

evidence supports the conclusion that low coverage presents the best conditions for delocalization (see above). Another issue is the presence of subsurface sites, which are of comparable energies with the surface sites and are thermally accessible. These sites, which are not visible to helium scattering, might influence the symmetry of the surface phase[19].

In summary, the vibrational states for H,D, and T on the Pd(111) surface were reported. A notable feature of these states is their anharmonicity, which is most prominent in the weak isotopic dependence of the parallel vibrational state (see Table I). The pooriness of harmonic estimates of the energies also demonstrates the importance of anharmonic effects. Harmonic estimates of the energy of the E state of H are off by 90 meV. Harmonic estimates do better for the  $A_1^1$  state and get better with increasing mass (see Fig. 2). The states have a large zero point energy, so it is not surprising that anharmonic regions of the potential energy surface are important. The ground state energy for H and the excited state energies for all three isotopes (see Table I) are greater than the classical barrier between sites, 175 meV. That these states can have a high energy relative to a barrier in one coordinate and still remain largely localized on one side of this barrier is due to the multidimensional nature of these states. For a discussion of the localization and zero point/barrier energy ratio in the context of clusters see Ref. [37]. The bandwidths of the states are narrow and an analysis of the coupling of the hydrogen eigenstates to the phonons indicates that the hydrogen only induces small lattice distortions (with an amplitude  $< 0.1 \text{ \AA}$ ) and that the hydrogen is localized on a particular binding site for a time scale on the order of a hundred picoseconds or more. The dynamics of hydrogen as it diffuses across the surface and also into the subsurface will be the subject of future study[40].

That anharmonic effects are more important for the computed perpendicular vibration (transitions to the E state) than the parallel vibration (transitions to the  $A_1^1$  state) could lead to some atypical HREELS results. HREELS finds that the the parallel frequency,  $\omega_{\parallel}$ , is less than the perpendicular,  $\omega_{\perp}$ , for the H isotope[17]. Since the perpendicular

mode has a stronger isotopic dependence than the parallel, it is possible that the ordering of the frequencies could change for heavier hydrogen isotopes and  $\omega_{\parallel}$  could become higher than  $\omega_{\perp}$ , although the present calculations find  $\omega_{\perp} < \omega_{\parallel}$  for all isotopes. An HREELS study of H and D on Pd(111) could resolve some of the issues discussed in this letter, including the ordering of the parallel and perpendicular vibrations and the isotopic dependence of these frequencies. Furthermore, the HREELS spectra could determine whether the excited states have bandwidth which is much larger than HREELS resolution (about 1 meV) or of the same magnitude as we are predicting here.

**Acknowledgements.** The authors are pleased to acknowledge the assistance of Dr. Diane Lynch, Dr. Lawrence Pratt, and Professor K. Birgitta Whaley. We would also like to thank NSF for its support of the present work through grant CHE 9203498.

## References

1. See, for example, K. Christmann, Surf. Sci. Rep. **9** (1988) 1.
2. In 1958, Eigen and De Maeyer proposed a now out of favor "protonic semiconductor" model for hydrogen in ice crystals. M. Eigen and L. De Maeyer, Proc. Roy. Soc. A **247** (1958) 505.
3. K. Christmann, R.J. Behm, G.Ertl, M.A. Van Hove, and W.H. Weinberg, J. Chem. Phys. **70** (1979) 4168.
4. M.J. Puska, R.M. Nieminen, B. Chakraborty, S. Holloway, and J.K. Nørskov, Phys. Rev. Lett. **51** (1983) 1081; M.J. Puska and R.M. Nieminen, Surf. Sci. **157** (1985) 413.
5. O. Grizzi, M. Shi, H. Bu, J.W. Rabalais, R.R. Rye, and P. Nordlander, Phys. Rev. Lett. **63** (1989) 1408.
6. C. Astaldi, A. Bianco, S. Modesti, and E. Tosatti, Phys. Rev. Lett. **68** (1992) 90.
7. C.M. Mate and G.A. Somorjai, Phys. Rev. B **34** (1986) 7417.
8. C-H Hsu, B.E. Larson, M. El-Batanouny, C.R. Willis, and K.M. Martini, Phys. Rev. Lett. **66** (1991) 3164.
9. M. El-Batanouny, private communication.
10. S.M. George, A.M. DeSantolo, and R.B. Hall, Surf. Sci. **159** (1985) L425; D.A. Mullins, B. Roop, and J.M. White, Chem. Phys. Lett. **129** (1986) 511; T-S Lin and R. Gomer, Surf. Sci. **225** (1991) 41.
11. R. DiFoggio and R. Gomer, Phys. Rev. B **25** (1982) 3490; S.C. Wang and R. Gomer, J. Chem. Phys. **83** (1985) 4193; C. Dharmadhikari and R. Gomer, Surf. Sci. **143** (1984) 223; E.A. Daniels, J.C. Lin, and R. Gomer, Surf. Sci. **204** (1988) 129.
12. E.G. Seebauer, A.C.F. Kong, and L.D. Schmidt, J. Chem. Phys. **88** (1988) 6597.
13. E.G. Seebauer and L.D. Schmidt, Chem. Phys. Lett. **123** (1986) 129.
14. X.D. Zhu, A. Lee, A. Wong, and U. Linke, Phys. Rev. Lett. **68** (1992) 1862.
15. For theoretical examinations of the H/W(110) diffusion experiments, see K. Freed, J. Chem. Phys. **82** (1985) 5264; K.B. Whaley, A.

- Nitzan, and R.B. Gerber, J. Chem. Phys. **84** (1986) 5181; A. Auerbach, K.F. Freed, and R. Gomer, J.Chem. Phys. **86** (1987) 2356; Q. Niu, J. Stat. Phys. **65** (1991) 317; P.D. Reilly, R.A. Harris, and K.B. Whaley, J. Chem. Phys. **97** (1992) 6875.
16. P-A Karlsson, A-S Mårtinson, S Andersson, and P. Nordlander, Surf. Sci. **175** (1986) L759.
  17. H. Conrad, M. E. Kordesch, R. Scala, and W. Stenzel, J. Electron. Spec. and Relat. Phen. **38** (1986) 289 and H. Conrad, M. E. Kordesch, W. Stenzel, and M. Sunjic, J. Vac. Soc. Tech. A **5** (1987) 452.
  18. M.S. Daw and M.I. Baskes, Phys. Rev. B **29** (1984) 6443.
  19. T.E. Felter, S.M. Foiles, M.S. Daw, and R.H. Stulen, Surf. Sci. **171** (1986) L379.
  20. H. Conrad, G. Ertl, and E.E. Latta, Surf. Sci. **4** (1974) 435.
  21. J. Völkl, G. Wollenweber, K.-H. Klatt, and G. Alefeld, Z. Naturforsch. **26a** (1971) 922; see also J. Völkl and G. Alefeld, in *Diffusion in Solids: Recent Developments*, edited by A.S. Nowick and J.J. Burton (Academic Press, New York, 1975).
  22. N.W. Ashcroft and N.D. Mermin, *Solid State Physics* (Saunders College, Philadelphia, 1976).
  23. G.E. Kimball and G.H. Shortley, Phys. Rev. **45** (1934) 815 and M.J. Puska and R.M. Nieminen, Phys. Rev. B **29** (1984) 5382.
  24. D.M. Ceperley and B.J. Alder, Science, **231** (1986) 555.
  25. This mass dependence is seen in the tunneling probabilities for a number of systems, including rectangular and parabolic barriers. See R.P. Bell, *The Tunnel Effect in Chemistry* (Chapman and Hall, London, 1980).
  26. H. Ibach and D.L. Mills, *Electron Energy Loss Spectroscopy and Surface Vibrations* (Academic Press, New York, 1982).
  27. H. Conrad, R. Scala, W. Stenzel, and R. Unwin, J. Chem. Phys. **81** (1984) 6371.

28. A.D. Johnson, K.J. Maynard, S.P. Daley, Q.Y. Yang, and S.T. Ceyer, Phys. Rev. Lett. **67** (1991) 927; K.J. Maynard, A.D. Johnson, S.P. Daley, and S.T. Ceyer, Faraday Discuss. Chem. Soc. **91** (1991) 437.
29. A.M. Baró, H. Ibach, and H.D. Bruchmann, Surf. Sci. **88** (1979) 384.
30. H. Conrad, W. Stenzel and M.E. Kordes, presented at the 5th International Conference on Vibrations at Surfaces, Grainau, FRG, 1987, p. 0-3.
31. P.J. Feibelman and D.R. Hamann, Surf. Sci. **182** (1987) 411.
32. S. Andersson, Chem. Phys. Lett. **55** (1978) 185; P.A. Karlson, A.S. Mårtinsson, S. Andersson and P. Nordlander, Surf. Sci. **175** (1986) L759.
33. L.J. Richter, T.A. Germer, J.P. Sethna, and W. Ho, Phys. Rev. B **38** (1988) 10403.
34. C. Nyberg and C.G. Tengstål, Solid State Commun. **44** (1982) 251; Phys. Rev. Lett. **50** (1983) 1680.
35. B. Voigtländer, S. Lehwald, and H. Ibach, Surf. Sci. **208** (1989) 113.
36. D.R. Hamann and P.J. Feibelman, Phys. Rev. B **37** (1988) 3847.
37. T. Holstein, Ann. Phys. (N.Y.) **8** (1959) 325; **8** (1959) 343; C.P. Flynn and A.M. Stoneham, Phys. Rev. B **1** (1970) 3966.
38. The bandwidth is six times (not twice) the Hamiltonian matrix element,  $\langle \phi_a | H | \phi_b \rangle$ , because of the three-fold symmetry of the lattice.
39. S.W. Rick, D.L. Lynch, and J.D. Doll, J. Chem Phys. **95** (1991) 3506.
40. S.W. Rick, D.L. Lynch, and J.D. Doll, J. Chem Phys. (in press).

Table I. Band centers and band widths for the ground and two first excited vibrational states of the hydrogen isotopes on the Pd(111) surface, in meV, and the vibrational frequencies corresponding to the the  $A_1^0$  to E transition ( $\omega_{\parallel}$ ) and the  $A_1^0$  to  $A_1^1$  transition ( $\omega_{\perp}$ ), in  $\text{cm}^{-1}$ .

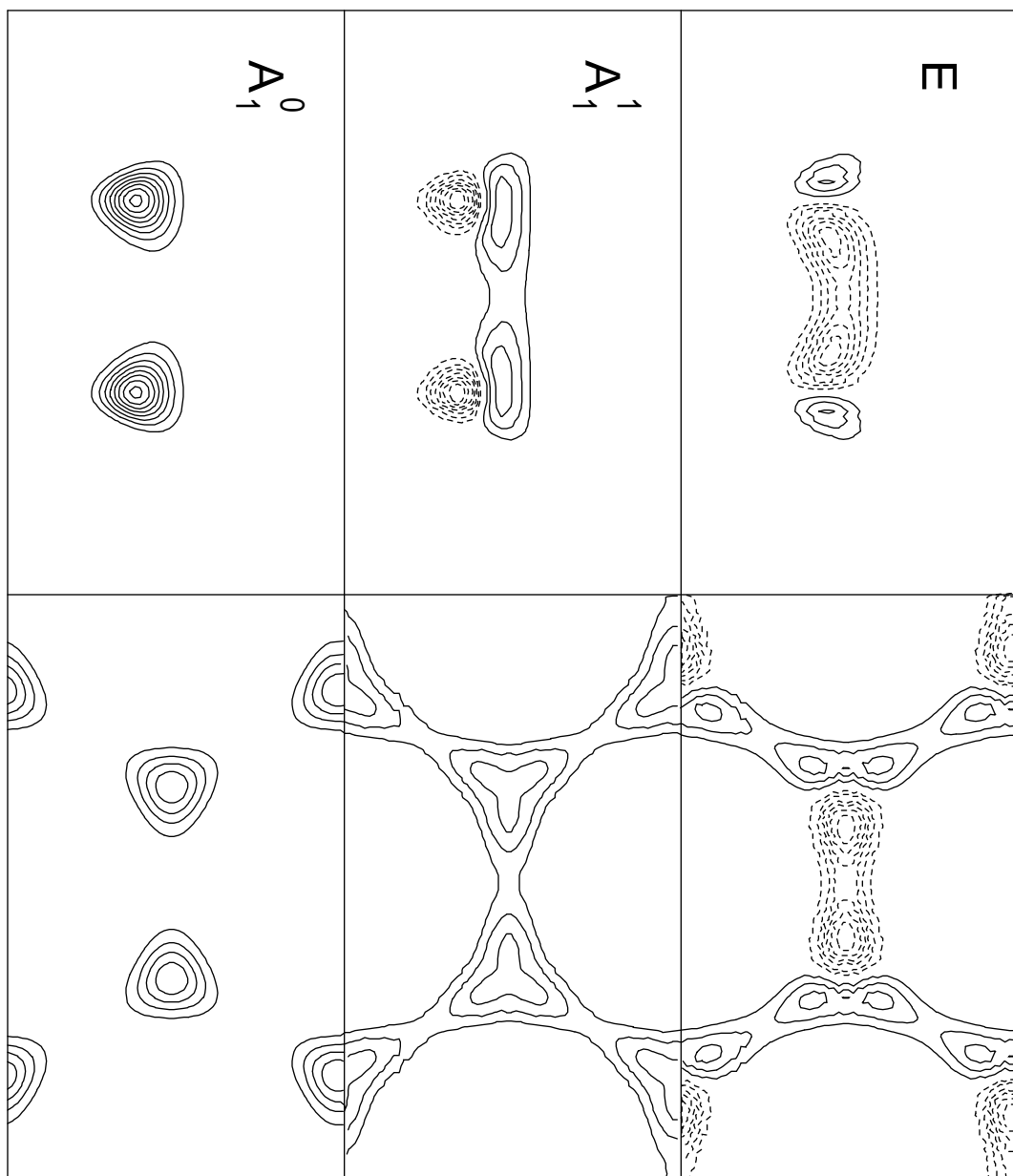
	H		D		T	
	Center (meV)	Width (meV)	Center (meV)	Width (meV)	Center (meV)	Width (meV)
$A_1^0$	236.3	0.011	169.2	0.000076	138.6	0.000004
$A_1^1$	345.9	2.17	252.5	0.023	208.2	0.0006
E	356.7	7.7	270.7	0.208	228.35	0.0075
Frequencies						
$\omega_{\parallel}/\text{cm}^{-1}$	971		819		724	
$\omega_{\perp}/\text{cm}^{-1}$	884		672		561	

### Figure Captions

Figure 1. Contours of the amplitudes of the  $\mathbf{k}=0$  bandstates for H/Pd(111) as a function of a surface coordinate and a coordinate perpendicular to the surface (left side) and as a function of the two surface coordinates (right side), for the E (top),  $A_1^1$  (middle), and  $A_1^0$  states (bottom). Each rectangle spans an area of  $2.75 \text{ \AA}$  by  $4.76 \text{ \AA}$  and the coordinate in the [111] direction begins at  $.02 \text{ \AA}$  below the surface plane. ■

Figure 2. Bandstate energies for H, D, and T, comparing the tight-binding state energies (the longer horizontal lines) to the harmonic estimates (the shorter horizontal lines).

[111] Direction



$[121]$  Direction

$[101]$  Direction



